

# Characteristic Based FVTD Computations for a Low Observable Configuration

Debojyoti Ghosh<sup>1</sup> Manoj B. Vaghela<sup>2</sup> Avijit Chatterjee<sup>3</sup>

Department of Aerospace Engineering  
Indian Institute of Technology Bombay  
Mumbai 400076, India

*Keywords:* Radar Cross-Section, Electromagnetics, Finite volume, Characteristics

## Introduction

Low observability requirements for aircraft subject to incident electromagnetic radiation are a low back-scatter for near-axial incident illumination. The target should also have a low return over a broad angular region. Low-observables are characterised by low specular reflection, and thus, greater contribution of creeping and travelling waves to the Radar Cross-Section (RCS).

Presently, there is lack of results and analysis for EM scattering by low-observable (LO) combat aircraft configurations in literature. Studies have been carried out for the VFY218 conceptual aircraft [1] but this aircraft cannot be classified as a LO configuration with relatively high returns for nose-on illumination (for example, an RCS of around 15 dBsm for HH polarization at 100 MHz). Similar attempts have been made to analyse the scattering by the F117 stealth fighter using the Fast Multipole Method (FMM) [2] in the VHF band. In the present study, the EM scattering and hence the RCS of a LO aircraft configuration is analyzed using a characteristic based finite volume time domain (FVTD) technique [3, 4]. The LO aircraft is the B2 "Advanced Technology Bomber" (ATB) [7] for which the surface geometry is modelled from information in literature and then the volume is discretized in a multi-block framework. The FVTD methodology is based on the Essentially Non-Oscillatory (ENO) technique from CFD and exploits the hyperbolicity of the Maxwell's equations (in total field form) to adapt CFD techniques to the CEM framework. The scattering from the aircraft in VHF and higher frequency bands for both horizontal and vertical polarization are computed and analyzed. Results are also presented for a LO test case, the metallic ogive, which constitutes a benchmark target accepted by the Electromagnetic Code Consortium (EMCC) [6].

The body of the aircraft has been assumed to be a perfect electric conductor (PEC). The geometrical features, like the blended wing-body, absence of protrusions, etc are observed to contribute to its low-observability but variations are seen for the RCS patterns between nose-on and broadside illuminations irrespective of the frequency or polarization.

## Governing Equations and Numerical Formulation

The Maxwell's equations, in conservative form, can be expressed as [3, 4]

$$u_t + f(u)_x + g(u)_y + h(u)_z = s \quad (1)$$

where  $u$  is the conservative variable,  $f$ ,  $g$  and  $h$  are the fluxes and  $s$  is the source term.

$$u = \begin{bmatrix} B_x \\ B_y \\ B_z \\ D_x \\ D_y \\ D_z \end{bmatrix}, f = \begin{bmatrix} 0 \\ -D_z/\epsilon \\ D_y/\epsilon \\ 0 \\ B_z/\mu \\ -B_y/\mu \end{bmatrix}, g = \begin{bmatrix} D_z/\epsilon \\ 0 \\ -D_x/\epsilon \\ -B_z/\mu \\ 0 \\ B_x/\mu \end{bmatrix}, h = \begin{bmatrix} -D_y/\epsilon \\ D_x/\epsilon \\ 0 \\ B_y/\mu \\ -B_x/\mu \\ 0 \end{bmatrix}, s = \begin{bmatrix} 0 \\ 0 \\ 0 \\ -J_x \\ -J_y \\ J_z \end{bmatrix}$$

$\mathbf{E}$  and  $\mathbf{H}$  are the electric and magnetic field intensity vectors respectively while  $\mathbf{D}$  and  $\mathbf{B}$  are the corresponding flux density vectors.  $\mathbf{J}$  is the impressed current density and  $\epsilon$  and  $\mu$  are the permittivity and permeability of the medium of propagation respectively.

<sup>1</sup> Under-graduate student, Email: ghosh@aero.iitb.ac.in, Phone: +91-22-25720011

<sup>2</sup> Research Associate, Email: manojv@aero.iitb.ac.in, Phone: +91-9819018209

<sup>3</sup> Asst. Professor (Corresponding Author), Email: avijit@aero.iitb.ac.in, Phone: +91-22-25767128

The scattered formulation is used to solve for the fields and the semi-discrete equation for propagation in free space can be written as

$$V_i \frac{d(u_i^{sc})}{dt} + \sum_{m=1}^M [(\mathbf{F}(u^{sc})) \cdot \hat{n} S]_m = 0; \quad \mathbf{F} = f\hat{i} + g\hat{j} + h\hat{k} \quad (2)$$

$M$  is the total number of cell faces, which in the present case, is six for hexahedral cells.  $V_i$  is the volume of the  $i$ th cell. The numerical flux function  $\mathbf{F}(u^{sc})$  is constructed using a second order ENO-Roe scheme [5]. Time evolution is through a two-stage TVD Kunge-Kutta procedure. Thus the algorithm is spatially and temporally second order accurate. Standard surface boundary conditions (zero total tangential electric field) are applied on the PEC surface and characteristic based boundary conditions are applied at the far-field boundary.

### Ogive (EMCC Benchmark)

Figure (1) shows the metallic ogive, a LO benchmark target of the Electromagnetic Code Consortium (EMCC) [6]. It has a half angle of 22.62 degrees, a half-length of 5 inches and a maximum thickness of 1 inch and discretized using an O-H topology in a single block. Results obtained using the FVT algorithm, as the variation of monostatic RCS with angle of incidence, are presented in figure (5), for a frequency of 1.18 GHz (vertical polarization), corresponding to an electric size of  $2\pi$  and good agreement can be seen with experimental results.

### Aircraft Surface Geometry and Grid Generation

The basic dimensions of the B2 ATB are 20.9 m length, 5.1 m height and 52.43 m wingspan [7]. However, accurate geometrical details of each part of the aircraft are not available due to its military sensitivity. A three view diagram in literature [7] was the basis of constructing the surface grid. Average dimensions of the cells were 0.9 mm in the longitudinal direction and 1.7 mm in the spanwise direction at the surface. The airfoil section chosen for the construction of the wings was E180, based on what is used in a radio-controlled model of this aircraft [8]. A clean configuration was chosen and control surfaces were included with the main body. The engine intake was assumed to be blocked and the surface perfectly conducting. Figure (2) shows the rendered surface of the aircraft.

The surface grid was generated by splitting the aircraft into twenty five blocks. Each surface block was a piecewise bilinear surface, formed by linear interpolation between boundary curves. These curves were formed as piecewise linear curves with sufficient resolution with point clustering near high curvature regions. Higher order interpolation was used to cluster grid cells near the body. The resulting volume grid was composed of fifty two blocks and approximately 1.5 million cells.

### Results

Computations are carried out at electric sizes of 545.8, 327.48 and 54.58, corresponding to the frequencies of 500 MHz, 300 MHz and 50 MHz for the actual full-sized aircraft, for both horizontal and vertical polarization. Analysis for the F-117 using the FMM has also concentrated in a similar frequency range (50MHz, 100MHz and 215.38 MHz for the full-scale aircraft) [2].

Figures (3) and (4) show the surface currents on the surface of the body for vertical polarization, at nose-on and broadside incidences at 300 Mhz. It is observed that for nose-on incidence, the leading edge of the wings and the engine intakes are the major contributors to the back-scatter. However, for broadside incidence, the fuselage acts the major contributor. Figure (6) and (7) compares the bistatic RCS variation for nose-on and broadside incidences at 300 MHz for VV and HH polarizations respectively. The EM scattering for the LO configuration is being analyzed at different incidence angles to find the angle corresponding to maximum back-scatter, as was found for the F117 as 68 degrees for HH polarization and between 70-105 degrees for VV polarization in the frequency bands considered [2]. Computations are also planned at higher frequencies with a finer grid.

## References

1. J.M. Song, C.C. Lu, W.C. Chew and S.W. Lee, *Fast Illinois Solver Code (FISC)*, IEEE Antennas and Propagation Magazine, Vol. 40, No. 3, 1998
2. J. Li, L. Li, T. Yeo and Y. Gan, *Radar Cross Section of Aircraft F117: Computation using Fast Multipole Method and Measurement using Compact Range*, pre-print
3. A. Chatterjee and A. Shrimai, *Essentially Non-Oscillatory finite volume scheme for electromagnetic scattering by thin dielectric coatings*, AIAA Journal, Vol. 42, No. 2, 2004
4. A. Chatterjee and S.P. Koruthu, *Characteristic based FVTD scheme for predicting electromagnetic scattering by aerospace configurations*, Journal of The Aeronautical Society of India, Vol. 52, No. 3, 2000
5. C.W. Shu and S. Osher, *Efficient implementation of essentially non-oscillatory shock capturing schemes II*, Journal of Computational Physics, Vol. 83, No. 1, 1989
6. A.C. Woo, H.T.G. Wang, M.J. Schuh and M.L. Sanders, *EM programmer's notebook-benchmark radar targets for the validation of computational electromagnetics programs*, IEEE Antennas and Propagation Magazine, Vol. 35, No. 1, 1993
7. *Jane's All The World's Aircraft*, 1991-1992, Jane's Information Group, Page 458 - 459
8. Airfoil section - [www.rcsail.com/B2s.htm](http://www.rcsail.com/B2s.htm)

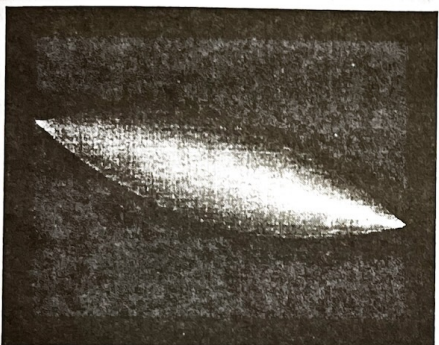


Figure 1: Rendered surface of ogive

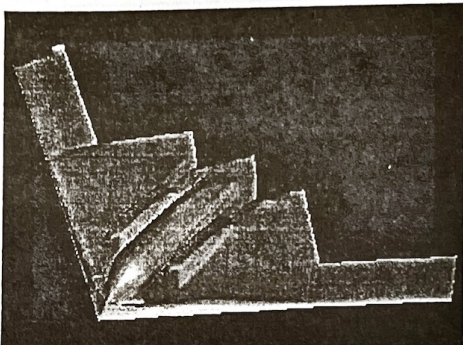


Figure 2: Rendered surface of B2

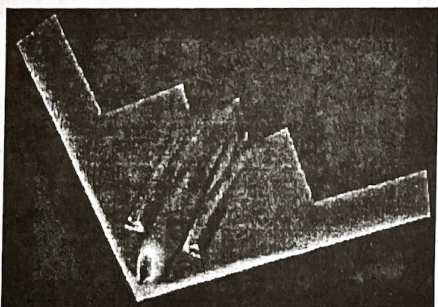


Figure 3: Surface currents at nose-on incidence

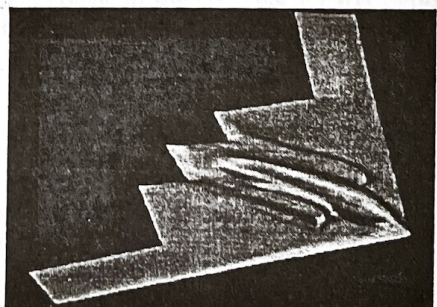


Figure 4: Surface currents at broadside incidence

Received: December 2006; Accepted: June 2007  
 © 2007 Department of Mathematics and Computer Science, Faculty of Engineering,  
 Babol University of Technology, Babol, Iran.  
 Corresponding author: Dr. Farzad Ebrahimi, Department of Mathematics and Computer Science,  
 Babol University of Technology, Babol, Iran.  
 E-mail: ebrahimi@ut.ac.ir

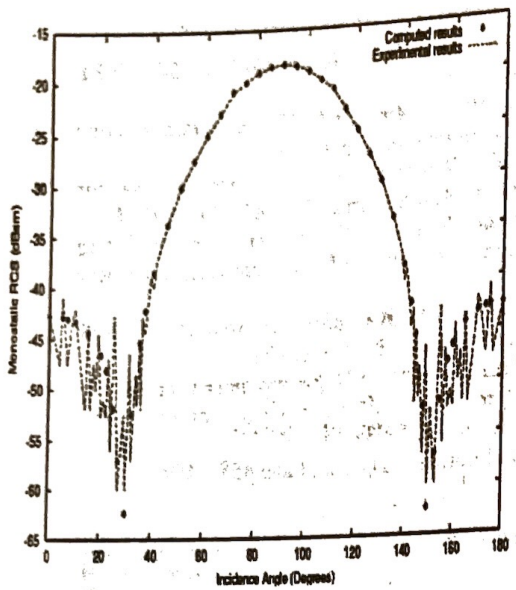


Figure 5: Monostatic RCS of a metallic ogive at 1.18 MHz (VV Polarization)

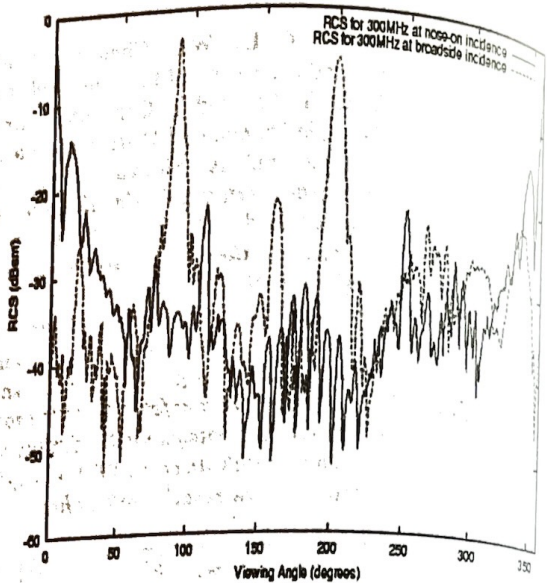


Figure 6: Bistatic RCS at 300 MHz (VV Polarization)  
(Back-scatter at 180 degrees for nose-on and 270 degrees for broadside incidences)

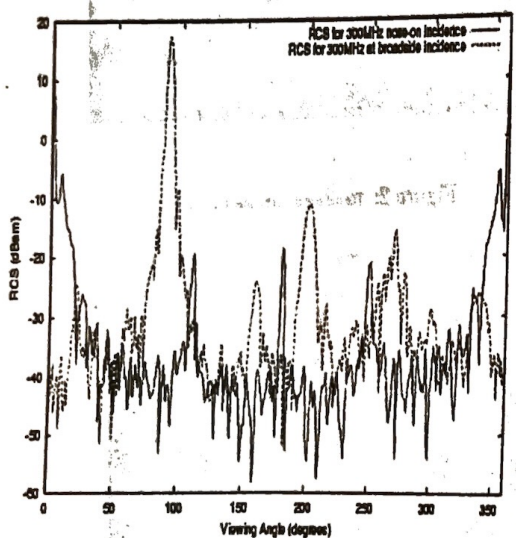


Figure 7: Bistatic RCS at 300 MHz (HH Polarization)  
(Back-scatter at 180 degrees for nose-on and 270 degrees for broadside incidences)

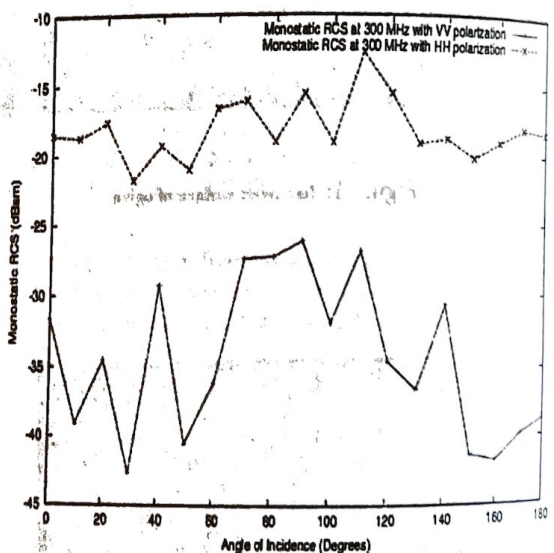


Figure 8: Monostatic RCS at 300 MHz (Nose at 0 degrees) (Data points at 10 degrees interval)



**7<sup>th</sup> Annual CFD Symposium  
CFD Division of AeSI  
PROCEEDINGS**

**August 11<sup>th</sup> and 12<sup>th</sup>, 2004**

**S. R. Valluri Auditorium  
National Aerospace Laboratories  
Bangalore - 560 017**